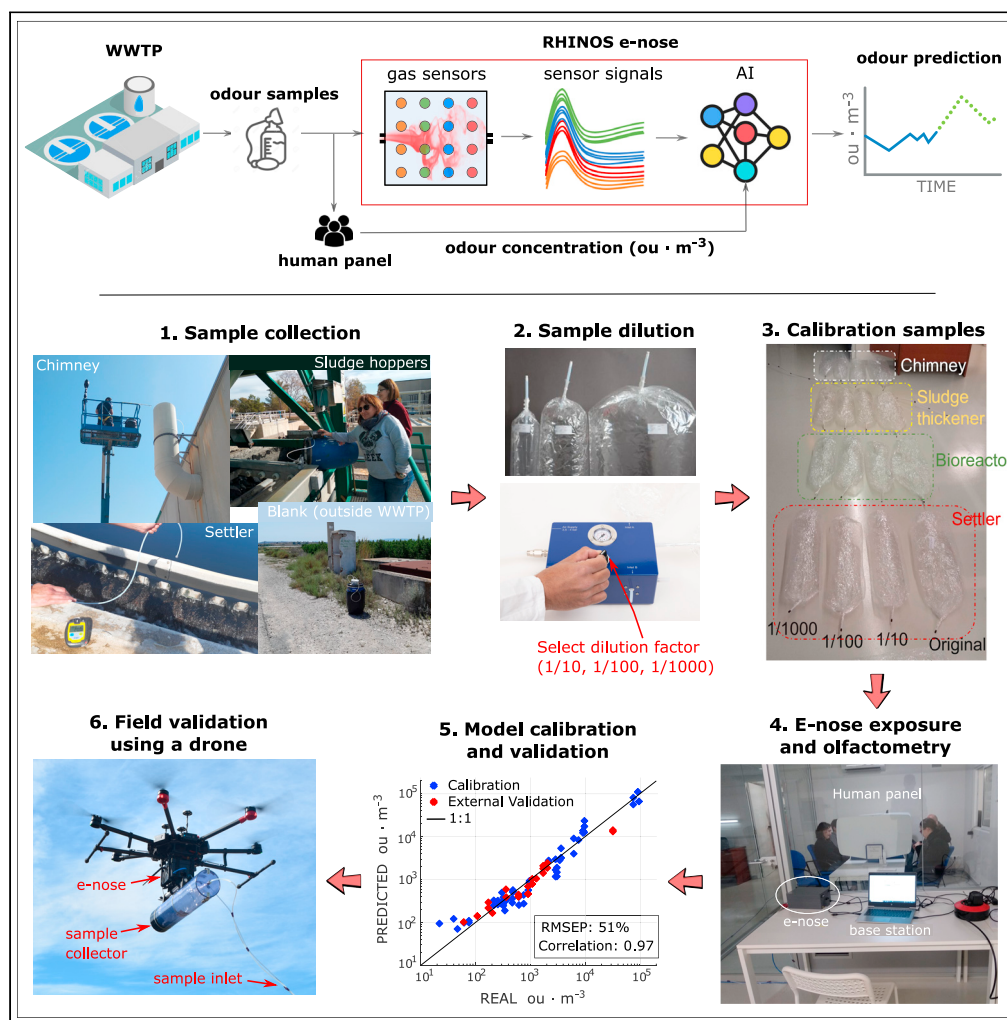**Article**

# RHINOS: A lightweight portable electronic nose for real-time odor quantification in wastewater treatment plants

Javier Burgués, María Deseada Esclapez, Silvia Doñate, Santiago Marco

smarco@ibecbarcelona.eu

Highlights

A portable e-nose for real time odor quantification according to EN13725 is described

The e-nose is installed on a small drone for dense spatial measurements

The e-nose is demonstrated and validated in a wastewater treatment plant

Errors in odor quantification are only slightly worse than dynamic olfactometry

## Article

# RHINOS: A lightweight portable electronic nose for real-time odor quantification in wastewater treatment plants

Javier Burgués,[1,2] María Deseada Esclapez,[3] Silvia Doñate,[3] and Santiago Marco[1,2,4,*]

## SUMMARY

**Quantification of odor emissions in wastewater treatment plants (WWTPs) is key to minimize odor impact to surrounding communities. Odor measurements in WWTPs are usually performed via either expensive and discontinuous olfactometry hydrogen sulfide detectors or via fixed electronic noses. We propose a portable lightweight electronic nose specially designed for real-time odor monitoring in WWTPs using small drones. The so-called RHINOS e-nose allows odor measurements with high spatial resolution, and its accuracy is only slightly worse than that of dynamic olfactometry. The device has been calibrated using odor samples collected in a WWTP in Spain over a period of six months and validated in the same WWTP three weeks after calibration. The promising results obtained support the suitability of the proposed instrument to identify the odor sources having the highest emissions, which may give a useful indication to the plant managers as regards odor control and abatement.**

## INTRODUCTION

Odor annoyance due to industrial gas emissions from wastewater treatment plants (WWTPs) is a recurring problem that is difficult to manage properly, partly due to the lack of appropriate instrumentation to accurately quantify odor concentrations in situ and in real time (Bourgeois et al., 2003; Lebrero et al., 2011; Van Harreveld, 2012). Such measurements are key to regularly verify the efficiency of odor abatement systems (Munoz et al., 2010), identify the main odor sources within the plant (Zarra et al., 2008), and predict off-site impacts based on atmospheric dispersion models (Naddeo et al., 2012; Stuetz and Frechen, 2001). When odors are exclusively measured by olfactometry (human panels), the high cost and discontinuous nature of this technique inevitably leads to an insufficient number of measurements to provide a representative characterization of the odor emissions. When instrumental measurements are based only on surrogate odor parameters, such as hydrogen sulfide ($H_2S$) or ammonia ($NH_3$), the presence and non-linear interactions between the different odorants in the mixture are ignored, leading to poor correlations with the odor concentration (Cangialosi et al., 2018; Franke et al., 2009; Lehtinen and Veijanen, 2011; Stuetz and Frechen, 2001). Among the different ways to express odor concentration, in this article we will use the "European odor units per cubic meter" ($ou_E \cdot m^{-3}$) as per the European standard EN13725:2003 (CEN, 2003).

Electronic noses (e-noses), also called sensor arrays or instrumental odor monitoring systems (IOMS), are currently considered the most promising tools for environmental odor monitoring (Bax et al., 2020; Capelli et al., 2014). An e-nose is a chemical measurement system based on an array of unspecific chemical sensors (typically 5–20 sensors) with complementary sensitivities to a wide range of volatile organic compounds (VOCs) and inorganic gases (Gardner and Bartlett, 1999). Most dominantly used sensors in the field of environmental monitoring are metal oxide semiconductors (MOS or MOX), although more and more frequently current systems include additional semi-specific sensors (e.g., electrochemical cells) for $H_2S$ or $NH_3$ (Alferes et al., 2017; Naddeo et al., 2016; Qu et al., 2008). By considering the odor mixture as a whole and not by its individual components, e-noses can produce better correlation with the odor concentration than any other instrumental method. For that, a pattern recognition (PR) algorithm must be calibrated with parallel olfactometric measurements to find the best possible mapping between the multivariate sensor signals (predictors) and the olfactometric measurement (predictand). After the e-nose is calibrated, it can be deployed on-site to continuously predict the odor concentration of new samples. The applicability of e-noses for continuous odor monitoring has been demonstrated in different industrial scenarios, including WWTPs

[1]Institute for Bioengineering of Catalonia (IBEC), The Barcelona Institute of Science and Technology, Baldiri Reixac 10-12, 08028 Barcelona, Spain

[2]Department of Electronics and Biomedical Engineering, Universitat de Barcelona, Marti i Franqués 1, 08028 Barcelona, Spain

[3]Depuración de Aguas del Mediterráneo (DAM), Avenida Benjamín Franklin 21, Parque Tecnológico, 46980 Paterna, Spain

[4]Lead contact

*Correspondence:
smarco@ibecbarcelona.eu

https://doi.org/10.1016/j.isci.2021.103371

(Alferes et al., 2017; Bottomley, 2010; Haas et al., 2008; Stuetz et al., 1998, 1999), landfills (Cangialosi et al., 2018), animal farms (Romain et al., 2013), composting plants (Mantovani et al., 2011; Sironi et al., 2007), and petrochemical plants (Zarra et al., 2021). In these cases, e-noses were typically installed at the outlet of odor control systems (e.g., deodorization chimneys) to monitor their efficiency in real-time (Alferes et al., 2017; Haas et al., 2008) or to provide continuous data to atmospheric dispersion models used to predict the off-site impact (Bottomley, 2010). In some exceptional cases, e-noses have been installed at the plant's fence line (Cangialosi et al., 2018) or even at the receptors (Capelli et al., 2008).

While fixed e-nose installations are highly interesting because of the continuous odor measurements they can provide, such measurements are only representative of a small measurement point located around the e-nose inlet. This is not a problem when the e-nose is installed at the outlet of ducted (channeled) emissions because the odor is confined in a small channel where the e-nose inlet can be conveniently placed. However, when the goal is to characterize the odor emissions in larger areas or in an entire plant, the highly localized measurements provided by a fixed e-nose are clearly insufficient. In these cases, data from many measurement locations are needed. An exhaustive coverage of an industrial installation using fixed e-noses would be unfeasible because of economic and practical reasons. Not only because of the sheer size of these facilities but also because an important part of the odor emissions come from area sources (e.g., settlers, bioreactors, compost piles), which cannot be monitored from a single measurement location, or from fugitive sources (e.g., leaks, openings in buildings, trucks loaded with sludge) that cannot be anticipated. According to a relatively recent market study (Schwarzböck, 2012), costs for a commercial e-nose system suitable for field monitoring range from 12 k€ to 48 k€, or even more depending on the configuration and additional devices (e.g., preconcentrators, filters, etc). An equal amount is typically required for the initial calibration of the device. For software allowing data analysis, additional costs must be considered (up to ∼10 k€ or annual fees). Maintenance and recalibration costs must also be considered.

A low-cost and versatile solution that has not been seriously investigated for industrial odor monitoring is portable e-noses. A portable e-nose is convenient because with a single device one could monitor the odor concentration in several locations of the plant, thus saving costs and reaching measurement locations unsuitable for fixed e-noses. For example, such an instrument can be used in walkover odor surveys whereby many measurements are taken at different spatial locations with the resulting concentrations being plotted on a map to provide a visual indication of the main odor hotspots and the sources having the highest emissions in terms of odor concentration. This may give a useful indication to the plant managers on where to concentrate their efforts for further monitoring or odor abatement. Until now, this type of map has been only possible via $H_2S$ measurements with portable hand-held detectors (Stuetz and Frechen, 2001) or with portable analyzers mounted on a drone (Burgués et al., 2021). The estimation of odor concentration in the field with a portable e-nose is currently an open problem. One of the main reasons why portable e-noses are rarely applied for field odor measurements is that the few commercial devices available in the market are lab-based units mostly intended for quality control in the food, beverage, and perfume industries. Previous studies that evaluated the feasibility of these commercial systems for real-time odor monitoring in industrial sites highlighted their poor performance when taken out of the laboratory (Jennings and Cox, 2002; Nake et al., 2005; Schwarzböck et al., 2012). Long response times, sophisticated measurement cycles requiring purging of the sensing chamber with reference to clean air, extensive sample preparation, and influence of environmental temperature and humidity were some of the alleged problems.

More promising results were obtained by Nicolas et al. (Nicolas et al., 2000) using a home-made e-nose for the simpler task of odor classification in various industrial sites (WWTP, printing shop, paint shop, and compost site). A discriminant analysis (DA) classifier trained with 52 odor samples and 25 clean air samples was used to predict in real time the odor class as the e-nose was moved to various spots around these sources. Qualitative conclusions about the e-nose performance for this task were drawn based on the temporal evolution of the discriminant functions. However, since no threshold was applied to the discriminant functions to declare if an odor was present of not, the typical figures of merit for a classification problem (e.g., false positive rate, confusion matrix) were not reported in this study. The lack of a rigorous statistical validation of the calibration models and the associated figures of merit is a common pitfall of many research studies involving e-noses (Boeker, 2014). Another weak point of these studies, also pointed out by Boeker et al., is the use of oversimplified datasets that do not capture the challenging conditions of field sampling. This has often led to overoptimistic claims about the potential performance of e-noses for in-situ odor
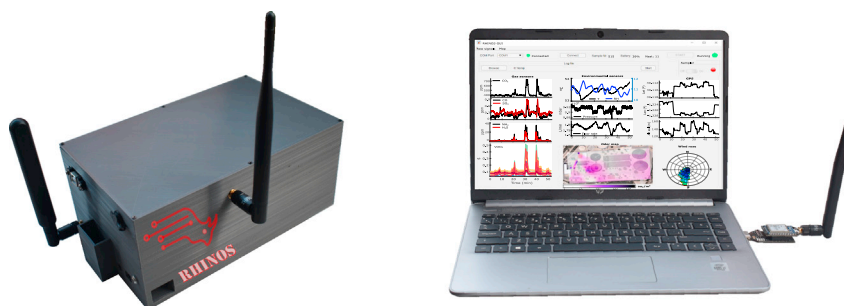
## iScience
### Article

**CellPress**
OPEN ACCESS



**Figure 1. RHINOS e-nose (left) and base station (right)**

sensing, not supported by follow-up validation studies. Only in very exceptional cases the predictions by an e-nose in the field have been validated with parallel olfactometric measurements. This is the case of the work by Alferes et al. (Alferes et al., 2017) in which the predictions by a commercial fixed e-nose installed at the outlet of a deodorization chimney in a WWTP were validated against nine olfactometric samples taken along the six weeks following calibration. The excellent qualitative agreement between both measurement methods, together with the fact that the main providers of environmental solutions are increasingly deploying e-noses in WWTPs and other industrial sites, suggests that e-noses can be indeed useful instruments for field monitoring.

Based on these motivations and in collaboration with one of the largest WWTP operators in Spain (Depuración de Aguas del Mediterráneo), we have developed a portable e-nose for odor quantification in WWTPs. The device, named RHINOS (Real-time HIgh-speed e-NOSe), can quantify odors in the range $50 - 10^5 ou_E \cdot m^{-3}$ with an average prediction error of a factor of two of the dynamic olfactometry value. It is lightweight (1325 g), low power (1 W), and integrates an on-board GPS receiver and wireless radio link to allow stand-alone operations either as a hand-held device or mounted on a remotely piloted aircraft system (RPAS) or small drone. In this article, we describe the architecture of the e-nose, the calibration and validation of the odor quantification model, and preliminary experimental results of the RHINOS mounted on a DJI Matrice 600 drone for a rapid assessment of industrial odors in a mid-sized WWTP in Spain.

## RESULTS AND DISCUSSION

### RHINOS electronic nose

The main outcome of the article is the portable e-nose RHINOS (Figure 1) tailored for real-time measurements of odorous compounds in WWTPs. Its main specifications are given in Table 1. The sensor suite includes 21 gas sensors of three technologies (metal oxide semiconductor, electrochemical cells, and nondispersive infrared) targeting the main odorous compounds of WWTPs such as hydrogen sulfide ($H_2S$), ammonia ($NH_3$), sulfur dioxide ($SO_2$), mercaptans, amines, short fatty chain acids, and other VOCs (Stuetz and Frechen, 2001). Two odorless gases, such as carbon dioxide ($CO_2$) and carbon monoxide (CO), are also measured due to their link to bacterial activity (Park and Craggs, 2010) and organic waste degradation (Haarstad et al., 2006), respectively. Environmental parameters such as temperature, relative humidity, pressure, and flow rate are continuously recorded inside the sensing chamber to either compensate their effect on the sensor signals (temperature and humidity) or detect failures in the fluidic system (pressure and flow rate). Other elements of this e-nose are a GPS receiver, internal SD card for data logging, and long-range point-to-point radio communication to send the measured data to a remote base station.

The internal architecture of the e-nose comprises electronic and fluidic subsystems (Figure 2). The electronic subsystem is based on a dual microcontroller (μC) architecture in which two μC are interconnected through a universal asynchronous receiver-transmitter (UART) port using a master-slave configuration. The master μC controls the electrochemical and NDIR sensors, the temperature, humidity, and pressure sensor, the GPS receiver, and the radio communication (see Table 2). These gas sensors are individually calibrated by the sensor manufacturer with temperature and humidity compensation via piecewise calibration functions programmed in the e-nose firmware. Each sensor is plugged into an analog front-end (AFE) socket which provides a complete signal path solution between the sensor and the microcontroller. The AFE module manages the installed gas sensor and converts the analog output signal (voltage or current) to a digital

**Table 1. Main specifications of the RHINOS e-nose**

| Parameter | Value |
|---|---|
| Gas sensors | 4 × Electrochemical cells (EC) for $NH_3$, $H_2S$, $SO_2$, CO <br> 1 × Nondispersive infrared (NDIR) for $CO_2$, <br> 16 × Metal oxide semiconductor (MOX) |
| Other sensors | Temperature, humidity, pressure, flow rate |
| Output signals | Raw data + calibrated output ($ou_E \cdot m^{-3}$) |
| Odor range | $50 - 10^5 ou_E \cdot m^{-3}$ |
| Prediction accuracy[a] | 50%–200% of reference value |
| Sampling frequency | 1 Hz (GPS disabled); 0.2 Hz (GPS enabled) |
| Flow rate | 1.8 L/min |
| GPS accuracy | $\pm 3$ m |
| Radio link | ZigBee 868 MHz (point-to-point) |
| Radio range | 2 km |
| Power consumption | 1 W |
| Main (external) battery | LiPo 3S 11.1V 5100 mAh |
| Internal battery | LiPo 2S 3.7V 500 mAh |
| Autonomy | 5 h of continuous measurements |
| Dimensions | $15 \times 25 \times 10$ cm$^3$ |
| Weight | 1325 g (incl. battery) |

[a]Standard deviation of relative errors in prediction

calibrated value. For that, the AFE module uses an integrated analog-to-digital converter (ADC) and the sensor-specific calibration parameters stored in a non-volatile EEPROM memory. The master µC periodically requests data to the slave µC through the UART interface, packs the received data with its own sensor data and GPS location, and sends it to the base station via a point-to-point radio link (ZigBee 868 MHz protocol). Table 3 shows the metal oxide sensors included the slave board. The TGS 2602 has high sensitivity to low concentrations of odorous gases, such as $NH_3$ and $H_2S$, which are the main markers of WWTP odors (Stuetz and Frechen, 2001). The TGS 2611 is relatively selective to methane ($CH_4$), a byproduct of the biological wastewater treatment processes (Campos et al., 2016). The TGS 2620 has high sensitivity to alcohols and organic solvent vapors (e.g., ketones), which can be found in wastewaters from pharmaceutical, textile, and paint-making industries (Modla and Lang, 2012).

Regarding the fluidic subsystem, all sensors are housed inside an optimized aluminum chamber with a miniature design (96 cm$^3$ internal volume) in which the gas sample is introduced at a constant flow rate
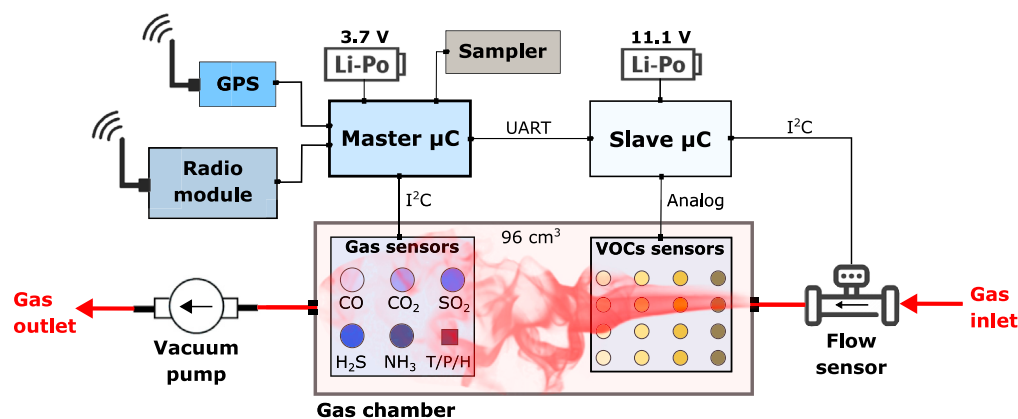


**Figure 2. Block diagram of the RHINOS e-nose hardware architecture**

## iScience
### Article

**Table 2. Specifications of electrochemical, NDIR and environmental sensors**

|  | Technology | Range | Accuracy | Response time ($T_{90}$) |
|---|---|---|---|---|
| Temperature | Integrated | −40 to +85°C | ±1°C | <2 s |
| Humidity | Integrated | 0 to 100% RH | ±3% RH | <2 s |
| Pressure | Integrated | 30 to 110 kPa | ±0.1 kPa | <2 s |
| Flow rate | Ultrasonic | −33 to +33 L/min | ±3% m.v. | <1 s |
| $CO_2$ | NDIR | 0 to 5000 ppm | ±100 ppm | <60 s |
| CO | Electrochemical | 0 to 100 ppm | ±0.5 ppm | <20 s |
| $H_2S$ | Electrochemical | 0 to 20 ppm | ±0.1 ppm | <20 s |
| $NH_3$ | Electrochemical | 0 to 100 ppm | ±0.5 ppm | <90 s |
| $SO_2$ | Electrochemical | 0 to 20 ppm | ±0.1 ppm | <45 s |

of 1.8 L/min by a diaphragm vacuum micropump sitting downstream of the chamber (Figure 3). The sensors, connectors, and screws are surrounded with polytetrafluoroethylene (PTFE) thread seal tape to ensure air-tight fitting. The chamber walls have been thinned to a few mm thickness (except around the screws and connectors) to further reduce the chamber weight to <200 g. All fluidic components are interconnected using PTFE tubing of 1/8' diameter. A digital flow sensor sitting at the inlet of the sensor chamber continuously monitors the flow rate of the input gas stream to detect any potential problem in the fluidic system (e.g., pump failure, gas leak, tubing obstruction).

The base station is a laptop computer with a USB antenna and a proprietary software with a graphical user interface (GUI) that allows the operator to visualize the e-nose signals in real-time, log the measured data, and plot the calibrated e-nose output ($ou_E \cdot m^{-3}$) as a 2D odor concentration map (Figure 4). Wind information coming from an in-situ anemometer can also be displayed. A button on the GUI allows the operator to remotely activate an odor sampling device connected to the e-nose in order to collect odor samples into polymer bags that can be analyzed by dynamic olfactometry to obtain ground truth for e-nose calibration and validation.

### Integration into a drone

The RHINOS e-nose has been especially designed to be used as a payload for small drones with limited payload capacity. A lightweight custom-made mounting plate (180 g) allows an easy installation in most

**Table 3. Specifications of the MOX sensors included in the slave board**

| Sensor | Model | Target gases | Heater voltage |
|---|---|---|---|
| M1 | TGS 2600 | $H_2$, CO, Ethanol | 1.6 V |
| M2 | TGS 2600 | $H_2$, CO, Ethanol | 3.2 V |
| M3 | TGS 2600 | $H_2$, CO, Ethanol | 4.0 V |
| M4 | TGS 2600 | $H_2$, CO, Ethanol | 4.9 V |
| M5 | TGS 2602 | $H_2S$, $NH_3$, Toluene | 1.6 V |
| M6 | TGS 2602 | $H_2S$, $NH_3$, Toluene | 3.2 V |
| M7 | TGS 2602 | $H_2S$, $NH_3$, Toluene | 4.0 V |
| M8 | TGS 2602 | $H_2S$, $NH_3$, Toluene | 4.9 V |
| M9 | TGS 2611 | $CH_4$, Hydrocarbons | 1.6 V |
| M10 | TGS 2611 | $CH_4$, Hydrocarbons | 3.2 V |
| M11 | TGS 2611 | $CH_4$, Hydrocarbons | 4.0 V |
| M12 | TGS 2611 | $CH_4$, Hydrocarbons | 4.9 V |
| M13 | TGS 2620 | Alcohols, ketones | 1.6 V |
| M14 | TGS 2620 | Alcohols, ketones | 3.2 V |
| M15 | TGS 2620 | Alcohols, ketones | 4.0 V |
| M16 | TGS 2620 | Alcohols, ketones | 4.9 V |
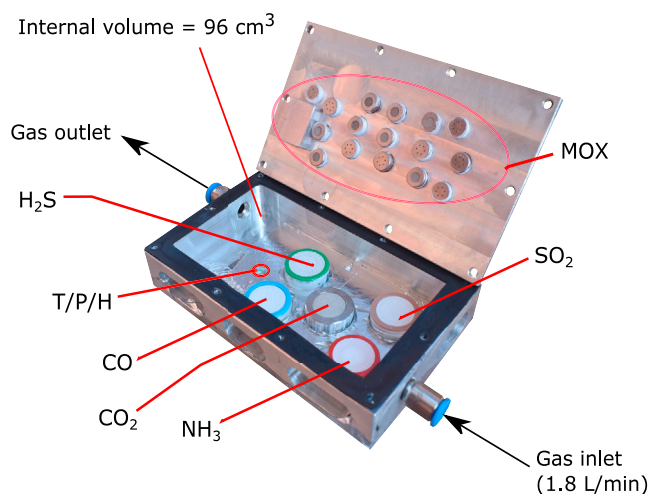
**Figure 3. RHINOS sensingchamber hosting 21 chemical sensors and a combo sensor for temperature, humidity, and pressure**

commercial drones (Figure 5). The piece, which is fabricated in acrylonitrile butadiene styrene (ABS) material, can hold payloads up to 10 kg and can also accommodate an odor sampling device for in-flight calibration and validation of the e-nose. As a proof of concept, we mounted the RHINOS into a DJI Matrice 600 drone for mapping the odor concentration in a WWTP. The inlet of the e-nose was connected to a 10-m PTFE tubing that hangs vertically from the drone to take samples without the influence of the turbulent downwash region produced by the propellers (Figure 6). A small weight (~150 g) is attached at the end of the tubing to keep it as stable as possible during flight. The required length of the tubing was determined by measuring the downwash with a hand-held anemometer placed below the fully loaded drone during hovering at multiple altitudes. The delay introduced by the tubing in the sample transport to the sensing chamber is compensated by the RHINOS firmware. The total weight of the payload including the e-nose, the mounting plate, and the tubing is ~1.8 kg.

**Test site**

A medium-sized WWTP in the south of Spain was used as the test site for the calibration and validation of the RHINOS e-nose. This plant has an extension of 35,000 $m^2$ and serves a population of 290,000 inhabitants. The sampling was performed around the four most problematic odor sources known by the plant managers: pretreatment building, settlers, bioreactors, and deodorization chimney (Figure 7). The latter one is located on the ceiling of the sludge dewatering building and corresponds to a chemical scrubbing tower (Alinezhad et al., 2019). This scrubber collects fumes from different parts of the plant (pre-treatment stage, sludge dehydration, sludge thickener, sludge storage building, and sludge hoppers) and filters them with a two-phase system involving NaClO and NaOH scrubbing (Chen et al., 2001; González-Sánchez et al., 2008) to reduce the amount of $H_2S$ gas released to the atmosphere.

A total of 31 odor samples were collected from these sources in three measurement campaigns spanning a period of 6 months (Table 4). Each source was sampled at three heights (0.5 m, 2 m, and 5 m) using a remotely operated vacuum sampler with capacity for 10-L Nalophan bags mounted on the DJI Matrice 600 drone. The sampling was randomized to reduce the contaminating effects of potential nuisance variables (e.g., ambient temperature, wind, operating regime of the plant). The obtained samples were stored in opaque containers and sent to a certified laboratory where they were analyzed by dynamic olfactometry in less than 30 h, complying with EN13725:2003.

Dynamic olfactometry was carried out using a T08 olfactometer (Odournet GmbH) configured with the "yes/no" method and four panelists. The uncertainty of the olfactometry measurements was estimated by the laboratory as a factor of two. After determining the odor concentration of a given sample, the remaining content in the bag was used for e-nose calibration and validation (See STAR Methods).
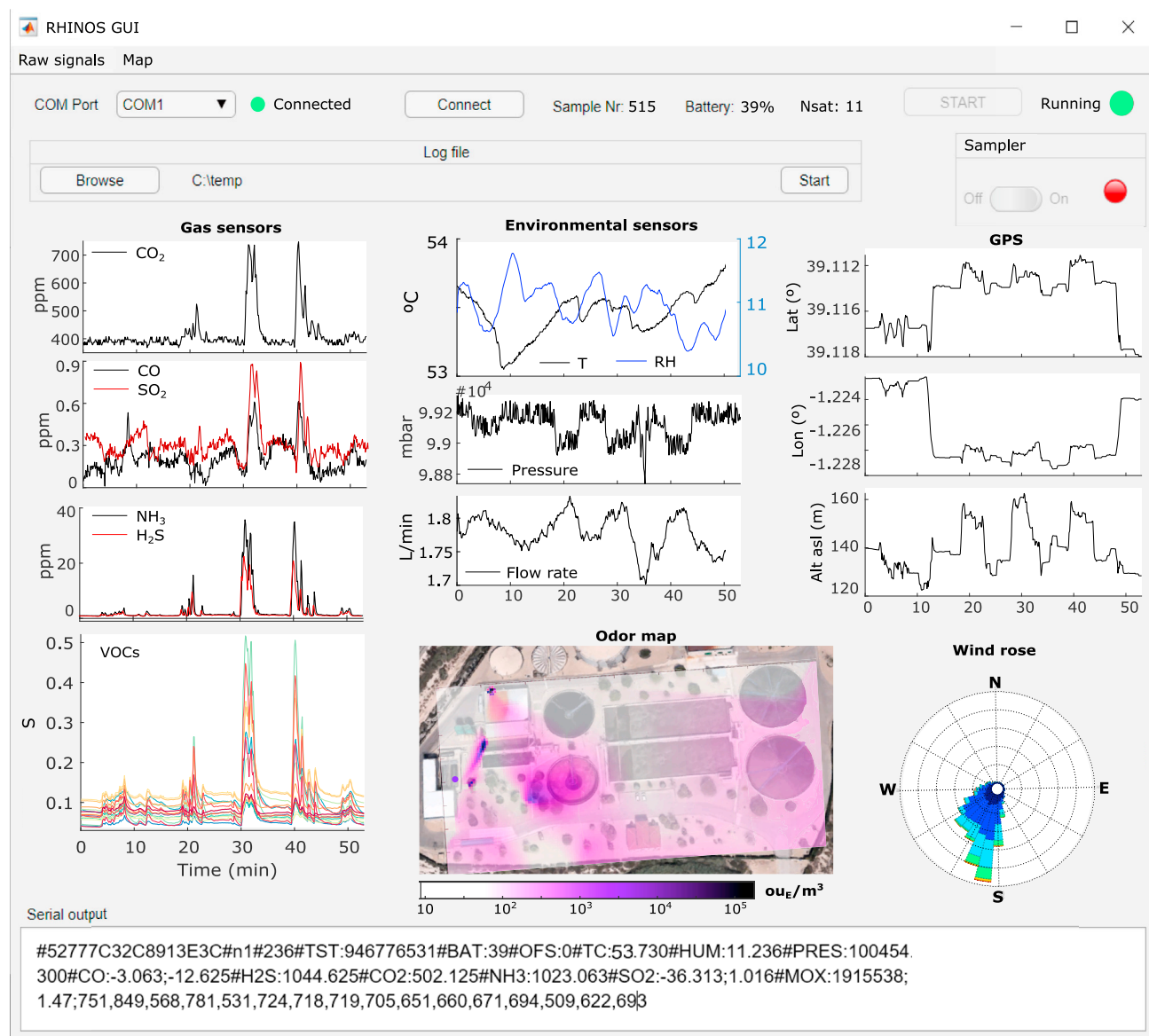
**Figure 4. Graphical user interface (GUI) running on the base station**

### E-nose response time

The response time is a key parameter of any mobile sensing system. The shorter the response time, the faster the sensing instrument can move without degrading the spatial resolution of the measurements. In an e-nose, the response time is normally dominated by the speed in filling and cleaning the sensing chamber. We measured the filling and cleaning time of the RHINOS chamber (see STAR Methods). As shown in Figure 8, a filling and cleaning time of ∼10 s can be observed in the signal of the miniPID connected to the exhaust of the chamber. The response of the $H_2S$ electrochemical sensor, also depicted in Figure 8, reveals a rise time for this sensor of ∼30 s regardless of the odor concentration, and a recovery time ranging from 40 to 60 s depending on the gas concentration. Since electrochemical sensors are slower than MOX and NDIR sensors, their response time will dominate the response time in our sensor array.

### Dynamic olfactometry results

The odor concentration of the original and diluted samples obtained in the three campaigns is listed in Table 5. For the original bags, it ranges from 40 $ou_E \cdot m^{-3}$ (bag 2-12, sample taken at 5 m above the

**Figure 5. Integration of the RHINOS e-nose underneath the DJI Matrice M600 drone using a custom payload bay**

deodorization chimney) to 96,653 $ou_E \cdot m^{-3}$ (bag 2-4, sample taken at 50 cm above the bioreactor surface). After diluting these bags, we had a total of 64 samples (56 odor samples +6 blanks) in the dataset. Among these, 40 of them (first and second campaigns) were used for model optimization and the remaining 24 (third campaign) for external validation. In general, there is a good coverage of the concentration range between 1 and $10^5 ou_E \cdot m^{-3}$ except in the range $10^4 - 10^5 ou_E \cdot m^{-3}$ which only contained one sample (bag 3-8). The chosen sampling heights and the coarse granularity of the dilution device made impossible to fill that concentration range with more samples.

### E-nose calibration and validation

Figure 9 shows the sequence of presentation of the samples and the corresponding MOX sensor signals during the first calibration experiment. A good correlation between the sensor responses and the odor concentration of the samples can be observed. We can also observe a fast stabilization and baseline recovery of the sensor signals, except for the highest concentrated odor sample where some of the sensors reached their saturation level.

We now compare the e-nose predictions to olfactometry, and how a model based only on the $H_2S$ sensor would perform (Figure 10). In the latter case we see a good correlation above $10^3 ou_E \cdot m^{-3}$ but limited sensitivity below this value. Despite 93% correlation was obtained, the average prediction error in external samples is 87% of the measured odor concentration. In contrast, the e-nose output has linear sensitivity in the range $50 - 10^5 ou_E \cdot m^{-3}$, higher correlation of 97%, and lower RMSEP of 51%. We can see that the worst predictions occur at concentrations $<50\ ou_E \cdot m^{-3}$ where the sensors operate near their LOD and dynamic olfactometry is more prone to errors, and in the range $10^4 - 10^5 ou_E \cdot m^{-3}$ where the only available sample was used for external validation. A Shapiro-Wilk test could not reject the null hypothesis of normal distribution of the residuals in the logarithmic scale (5% risk). The bias between the e-nose output and dynamic olfactometry is negligible and the 95% limits of agreement are [0.41×, 1.97×]. This intuitively means that roughly 95% of the predictions made by the e-nose will fall within this uncertainty band, regardless of the type of odor source. This is a remarkable performance considering that previous works reported major problems with quantification of odors from more than one source with the same predictive model (Stuetz et al., 1999). The performance obtained in our experiments is however difficult to benchmark against the literature because none of the works we are aware of have ever quantified the prediction error of an e-nose in external samples.

### Sensor importance for prediction

We studied the importance of each sensor in the array for odor prediction by computing the VIP scores of the PLSR model (Figure 11). Using the cut-off threshold of VIP = 1, the most relevant sensors are four specific sensors (mainly $H_2S$ and $NH_3$, followed by $SO_2$ and $CO_2$ and a subset of four non-specific MOX sensors (M1: TGS 2600 at 1.6 V, M3: TGS 2600 at 4.06 V, M6: TGS 2602 at 3.25 V, and M7: TGS 2602 at 4.06 V). The fact that the best predictive power is achieved by a combination of specific and non-specific sensors agrees with the results reported by Qu et al. during the analysis of samples from manure swings using a commercial e-nose with 32 non-specific conducting polymer (CP) sensors and two specific detectors for $H_2S$ and $NH_3$ (Qu et al., 2008). They found that combining the signals of the specific detectors with a subset of 3

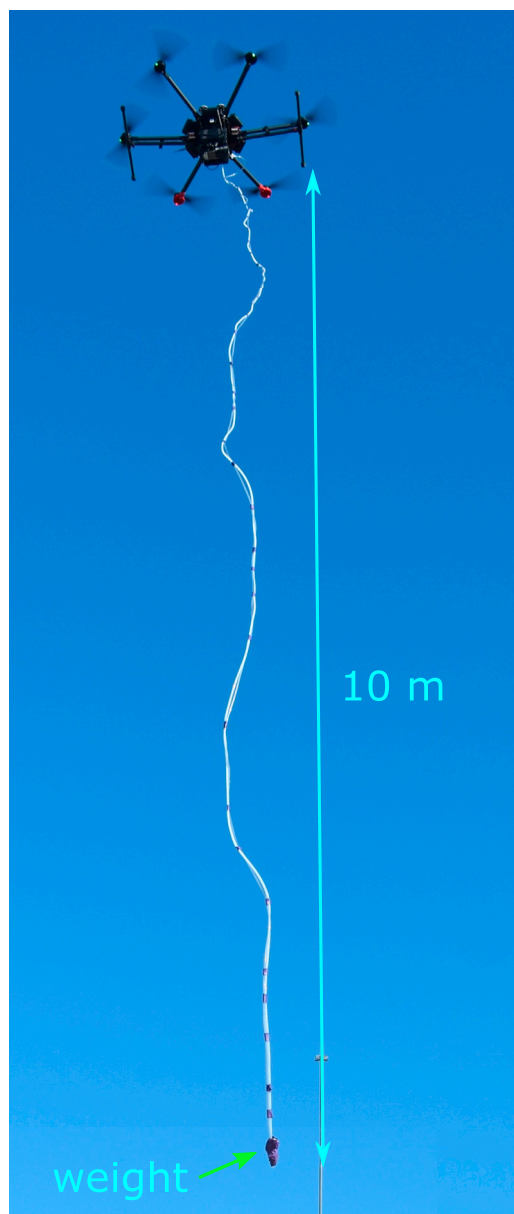## iScience
### Article

CellPress
OPEN ACCESS



**Figure 6. Final assembled system on flight using a 10-m weighted sampling tube**

CP sensors was more effective for predicting the odor concentration in external validation samples than using the CP sensors or the external detectors independently (R-squared of 0.75 vs 0.51). In our experiments, the combination may be advantageous because MOX sensors can compensate the reduced sensitivity of electrochemical sensors in the low concentration range. In this way, the calibration model can give more weight to the MOX sensors at low concentrations and rely more on the electrochemical cells at higher concentrations. It is also worth mentioning the relevant contribution of $CO_2$ sensor to the predictive model, which may be due to the correlation of $CO_2$ with bacterial activity in the biological treatment processes.

Regarding the importance of the different MOX sensor models included in the array, the TGS 2602 (targeting $H_2S$ and $NH_3$) and TGS 2600 (targeting ethanol and hydrogen) were considered the most relevant MOX sensor models, which agrees with the results obtained by Oliva et al. in an odor classification problem where the TGS 2602 achieved the highest correlation with the studied odor classes (refining plant, municipal solid waste, and coffee aroma) (Oliva et al., 2021). Regarding the operating voltage, it is surprising that the nominal voltage

**Figure 7. Aerial view of the WWTP used as test site, with the main odor sources highlighted in different colors**

recommended by the manufacturer (i.e., 5 V) was not considered optimum for odor prediction in our dataset. None of the TGS 2611 and TGS 2620 sensor units (sensitivity tuned to methane and organic solvents, respectively) was considered important by the model, which makes sense as methane is odorless and organic solvents may only be present in wastewater from specific industries such as painting houses.

Assessing which are the sensors with higher predictive importance not only allows for improving the model performance (i.e., by refitting the model only with the selected variables, thus reducing the overfitting due to noise generated by irrelevant features) but also to design tailored instrumental devices. In particular, the information provided in Figure 11 is very useful to reduce the size, weight, and power consumption of future versions of the RHINOS. Since MOX sensors dominate the power consumption of the e-nose, by removing 12 of them (i.e., the ones with lowest predictive power) we could save 75% of the power consumption, leading to an overall consumption of ~250 mW. Also, a smaller number of sensors could allow for a smaller and lighter sensing chamber with faster filling and cleaning time. The costs and maintenance of the e-nose will also benefit from a reduced sensor set.

### E-nose validation on the drone

Validation measurements with the RHINOS mounted on a small drone were carried out during the third campaign. Figure 12 compares the real-time odor predictions made by the e-nose and the parallel olfactometric measurements, both made at the same sampling location. In general, there is a good qualitative agreement between both measurement methods. In 10 out of 13 olfactometric measurements (~75%), the e-nose predictions lie within the uncertainty band of olfactometry. These results illustrate how important it is to validate the e-nose in the field, as the correlation observed in the field (72%) was considerably lower than the one obtained in the lab (97%). A drop in performance was expected because of the challenging conditions of field operation, most notably the fact of applying a calibration model developed for steady-state signals to predict odor concentration based on dynamic (transient) sensor signals. Nonetheless, the results are clearly better than our expectations. An interesting follow-up research question is if the field performance of the e-nose could be improved by calibrating it with real-time transient signals measured in the field rather than with steady-state signals obtained during exposure to odor bags.

### Conclusions

This paper has described the design of a portable e-nose for real-time odor quantification and demonstrated its application in a real WWTP. The developed prototype was able to predict real-time odor

**Table 4. Sampling plan used to collect odor samples for e-nose calibration and validation**

| Campaign | Date | # Samples | Sources | | | | | | |
|---|---|---|---|---|---|---|---|---|---|
| | | | BLK | MHL | PRE | BIO | SET | SLT | CHI |
| 1 | 28/01/20 | 5 | 2 | 1 | 0 | 1 | 1 | 1 | 0 |
| 2 | 25/06/20 | 13 | 2 | 0 | 3 | 3 | 3 | 0 | 3 |
| 3 | 15/07/20 | 13 | 2 | 0 | 3 | 3 | 3 | 0 | 3 |
| TOTAL | | 31 | 6 | 1 | 6 | 7 | 7 | 1 | 6 |

BLK, Blank; MHL, Manhole; PRE, Pretreatment; BIO, Bioreactor; SET, Settler; SLT, Sludge Thickener; CHI, Chimney.
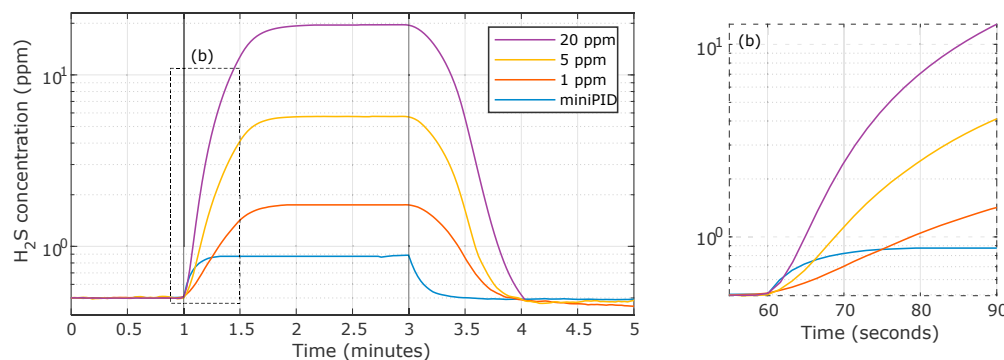
CellPress
OPEN ACCESS



**Figure 8. Characterization of the filling and cleaning time of the sensing chamber**
The blue trace is the response of a fast (<1 ms) photo-ionization detector (miniPID) placed at the exhaust of the chamber. The red, yellow, and purple lines are the responses of the $H_2S$ electrochemical sensor to three odor samples with increasing $H_2S$ concentration (1, 5, and 20 ppm). The vertical solid lines at t = 1 min and t = 3 min indicate the start and end of the odor exposure. (b) Is a zoom in of the area selected in the main plot.

concentration ($ou_E \cdot m^{-3}$) in the field three weeks after calibration with slightly worse accuracy than the reference method (dynamic olfactometry). This promising performance must be validated over longer time periods and under different operating and weather conditions to gain more confidence into its suitability for the intended application. Validation in other WWTPs would be also desirable to check the generalization capabilities of the PLSR predictive model implemented in the e-nose. The results obtained in this study encourages the development and application of portable e-noses to other industries concerned with odor problems, such as landfill sites, composting plants or livestock farms (Capelli et al., 2014).

This study also demonstrated that odor quantification from drone-based measurements is feasible with a dedicated e-nose and a sampling system that avoids the downwash from the propellers. Installing the e-nose on a drone allowed measuring in dangerous and hard-to-reach measurement locations, such as the deodorization chimney, without any human risk. The utility of drones for gas measurements was already demonstrated in a previous work where we used the same drone equipped with electrochemical sensors for mapping $H_2S$ concentration in a WWTP (Burgués et al., 2021). That work also demonstrated the potential capabilities of drone-mounted e-noses for odor source identification. The present work is the first reported attempt of estimation of odor concentration from drone measurements, and we expect many more works to come in this direction since the field of environmental gas sensing using small drones is growing exponentially (Burgués and Marco, 2020). A "flying e-nose" can become a powerful tool for environmental odor monitoring. In the short term, plant operators can use it for measuring odors in hard-to-reach or dangerous locations, identifying the major odor sources in their plants, or for mapping the odor concentration over vast (3D) areas. In a medium-term future, the above tasks could be carried out semi-autonomously (with limited human intervention) or fully autonomously thanks to map-based (Burgués et al., 2019) or bioinspired (Harvey et al., 2008; Lochmatter, 2010; Neumann et al., 2013) search strategies. For that to become a reality, more research on techniques to improve the performance of low-cost gas sensors is encouraged, especially in terms of response time, sensitivity (Dey, 2018; Wang et al., 2010), and power consumption (Burgués and Marco, 2018; Palacio et al., 2020).

In the longer term, portable e-noses could be used to obtain odor emission rates (OER), expressed in o.u./s, needed to feed atmospheric dispersion models that can predict off-site impact (Schauberger et al., 2011). While source-specific sampling methods, such as flux chambers, and complex mathematical models are currently required to estimate OERs (Frechen, 2004), odor concentration data could be used in combination with measured flow rates from point-like (channeled) sources and complex micrometeorological methods (Prata et al., 2021) to indirectly estimate OERs. This is an interesting line of research that is currently far from being state-of-the-art.

### Limitations of the study
The measurements presented in this paper were collected in a single WWTP during the first six months of the year; therefore, it is not easy to state how the e-nose would perform in other WWTPs or in other seasons.

*iScience*
Article

**Table 5. Set of bags used for calibration**

| Bag ID | Date | Source | Distance | Odor concentration ($ou_E \cdot m^{-3}$) | | | |
|--------|------|--------|----------|----------|------|-------|--------|
| | | | | Original | 1/10 | 1/100 | 1/1000 |
| 1–1 | 28/01/20 | Bioreactor | 0.5m | 76,111 | 7,611 | 761 | 76 |
| 1–2 | 28/01/20 | Sludge thickener | 0.5m | 6,222 | 622 | 62 | 6 |
| 1–3 | 28/01/20 | Settler | 0.5m | 2,165 | 216 | 21 | 2 |
| 1–4 | 28/01/20 | Influent manhole | 0.5m | 477 | 47 | 4.7 | 0.47 |
| 2–1 | 25/06/20 | Settler | 0.5m | 9,742 | 974 | 97 | – |
| 2–2 | 25/06/20 | Settler | 2m | 3,069 | – | – | – |
| 2–3 | 25/06/20 | Settler | 5m | 304 | – | – | – |
| 2–4 | 25/06/20 | Bioreactor | 0.5m | 96,653 | 9,665 | 966 | – |
| 2–5 | 25/06/20 | Bioreactor | 2m | 2,896 | 289 | – | – |
| 2–6 | 25/06/20 | Bioreactor | 5m | 483 | – | – | – |
| 2–7 | 25/06/20 | Pretreat | 0.5m | 3,444 | 344 | – | – |
| 2–8 | 25/06/20 | Pretreat | 2m | 323 | – | – | – |
| 2–9 | 25/06/20 | Pretreat | 5m | 256 | – | – | – |
| 2–10 | 25/06/20 | Chimney | 0.5m | 91,952 | 9,195 | 919 | 91 |
| 2–11 | 25/06/20 | Chimney | 2m | 3,649 | 365 | – | – |
| 2–12 | 25/06/20 | Chimney | 5m | 40 | – | – | – |
| 3–1 | 15/07/20 | Settler | 0.5m | 609 | 61 | – | – |
| 3–2 | 15/07/20 | Settler | 2m | 76 | – | – | – |
| 3–3 | 15/07/20 | Settler | 5m | 91[a] | – | – | – |
| 3–4 | 15/07/20 | Bioreactor | 0.5m | 1,722 | 172 | – | – |
| 3–5 | 15/07/20 | Bioreactor | 2m | 72[a] | – | – | – |
| 3–6 | 15/07/20 | Bioreactor | 5m | 912 | – | – | – |
| 3–7 | 15/07/20 | Chimney | 0.5m | 1,290 | – | – | – |
| 3–8 | 15/07/20 | Chimney | 2m | 32,254 | 3,225 | 322 | – |
| 3–9 | 15/07/20 | Chimney | 5m | 3,069[b] | – | – | – |
| 3–10 | 15/07/20 | Pretreat | 0.5m | 362 | – | – | – |
| 3–11 | 15/07/20 | Pretreat | 2m | 2,048 | 205 | – | – |
| 3–12 | 15/07/20 | Pretreat | 5m | 1,085 | 108 | – | – |

[a]Approximated. Not enough volume in the bag to complete the required olfactometry rounds.
[b]Approximated. Content of original bag was transferred to a second bag due to presence of leaks.

This is because the pattern of emissions in a WWTP is not stationary and there is large variability in the emissions depending on process factors (e.g., quality of influent water and flow rate) but also on environmental conditions (wind, temperature, humidity, precipitation, etc.). There are also seasonal trends. Thus, the recorded signals only represent the emissions during the time of sampling. Similarly, the emissions of two WWTPs can differ substantially based on the kind of treatment technologies used, the origin of the incoming water, the efficacy of the deodorization systems, and the influence of local temperatures and humidity, among many other factors. Probably, a calibration model developed in one WWTP will not produce accurate predictions when directly applied to another WWTP with slightly different characteristics. Recalibration of the e-nose using "calibration transfer" samples from the new site could be necessary to achieve good performance. The number of calibration samples can be reduced to a minimum using specific calibration transfer methodologies (Fernández et al., 2016; Fonollosa et al., 2016; Rudnitskaya, 2018). However, it is important to highlight that while those methods have been very successful in laboratory conditions, only few examples of their performance in the field have been reported (Deshmukh et al., 2014), and as far as we know they have not been yet applied to WWTPs.

On the other hand, due to the inherent drift and memory effect of low-cost gas sensors a calibration model built and tested on the same site can degrade its performance over time even if the emissions and
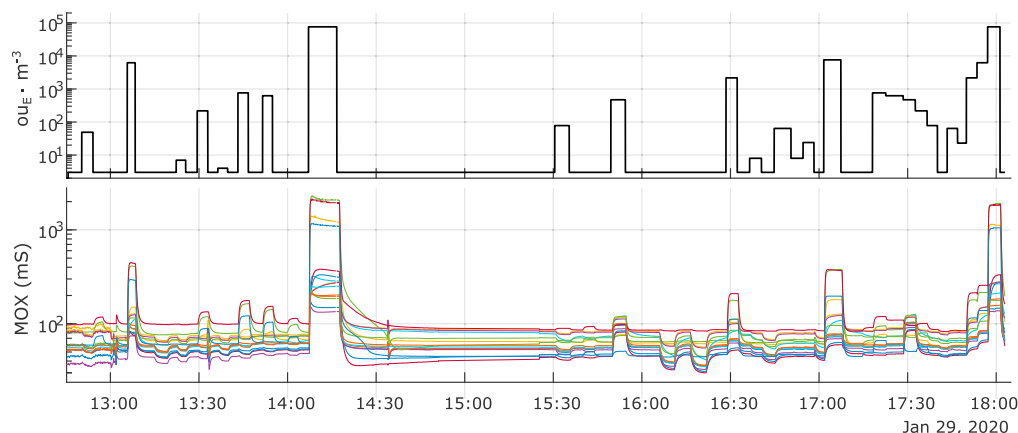
**Figure 9. Example of MOX sensor signals during the first campaign calibration experiment.**

environmental factors do not substantially change their characteristics (Bax et al., 2021). The reasons for sensor drift are comprehensively explained by Korotcenkov et al. (Korotcenkov and Cho, 2011) and there is an ample body of literature discussing drift counteraction techniques (Bax et al., 2021; De Vito et al., 2012; Di Carlo and Falasconi, 2012; Fonollosa et al., 2016; Marco et al., 1998; Padilla et al., 2010; Rudnitskaya, 2018; Yan and Zhang, 2016; Yi et al., 2021; Ziyatdinov et al., 2010).

Two limitations associated with the use of dynamic olfactometry as the reference method for instrument calibration is the high uncertainty associated to this technique and the limited number of samples that can be measured with a reasonable budget. The uncertainty of the reference method imposes a lower bound on the performance that can be achieved in the calibrated instrument. In the case of dynamic olfactometry as per standard EN 13725:2003, a factor of two errors can be expected, at the very minimum, in the predictions of any instrument calibrated against this method. The measurement uncertainty of olfactometry could significantly improve under the new olfactometric standard EN13725:2021 (to be published), especially with the introduction of new practices, such as the use of a wider range of reference odorant gases and paired environmental samples (Harreveld, 2021). It should also be noted that due to the inherent
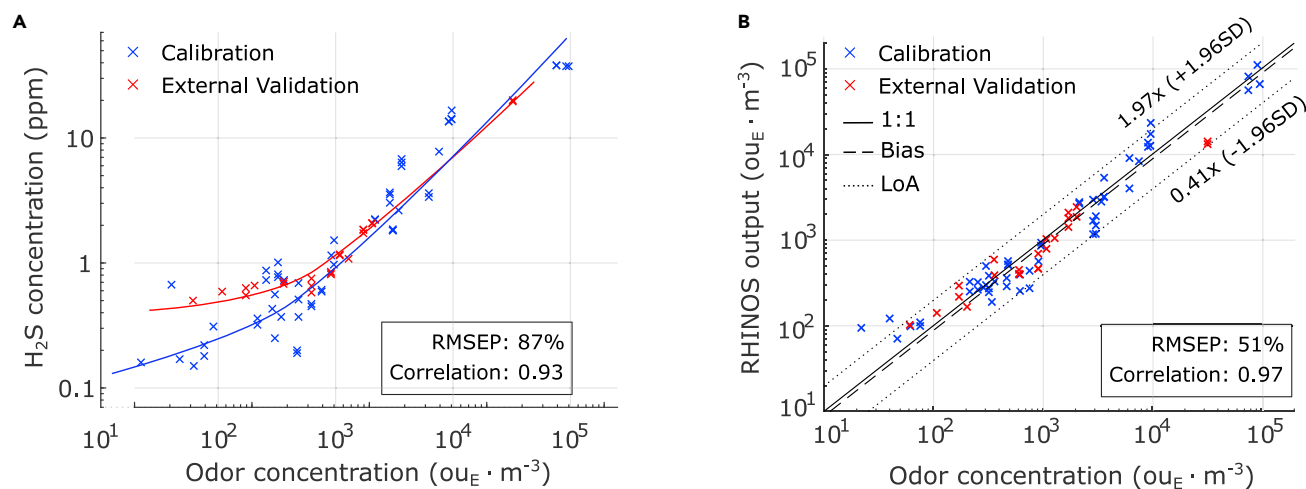


**Figure 10. Rhinos output provides a better estimation of odour concentration than H₂S concentration**

(A) H$_2$S concentration vs odor concentration (both in log scale). The solid lines represent polynomial fittings to the data. Blue crosses are calibration data and red crosses are external validation data.

(B) RHINOS output vs odor concentration (both in log scale). Blue crosses are calibration data and red crosses are external validation data. The bias and limit of acceptance (LoA) have been calculated using the Bland-Altman procedure. In both subplots, the indicated RMSEP and correlation are calculated with external validation samples. Bias is represented by a discontinuous line. Perfect agreement is represented by a solid line. Limits of acceptance are represented by a dotted line. Correlation with odor concentration improves using the full RHINOS output compared with a single H$_2$S measurement.
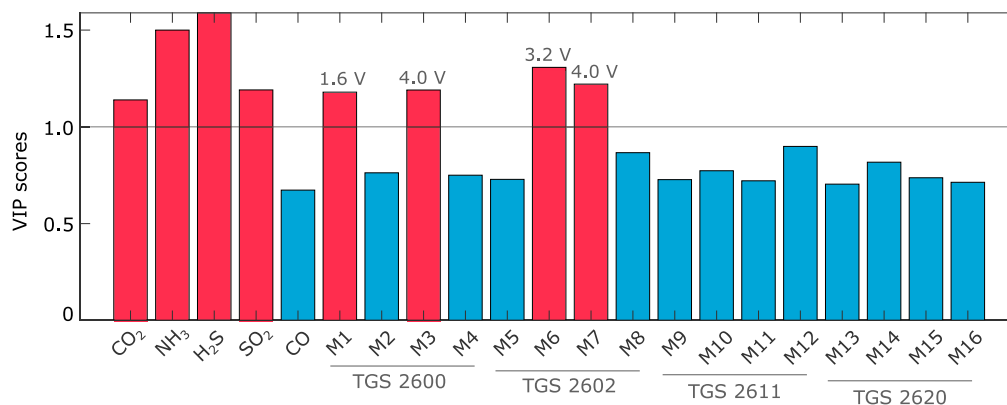
**CellPress**
OPEN ACCESS

*iScience*
Article



**Figure 11. Variable Importance in Prediction (VIP) scores of the 21 chemical sensors in the array**
Sensors with VIP>1 are highlighted in red and considered relevant for prediction.

instability of the calibration model of an e-nose, periodic recalibrations using dynamic olfactometry as ground truth will be necessary during the lifetime of the device. A limited number of olfactometric samples prevents the use of sophisticated calibration models, such as artificial neural networks (ANN), which could potentially provide improvements over traditional models such as PLS (Zarra et al., 2019). One possibility to deal with a low number of calibration samples is the use of semi-supervised learning (Zhu and Goldberg, 2009), by which a calibration model is trained with a combination of labeled and unlabeled samples. This technique has been already applied to e-nose data with preliminary good results (De Vito et al., 2012; Liu et al., 2014; Zhang et al., 2016).

The developed e-nose also has limitations for drone-based measurements because its response time ($\sim$30 s) limits considerably the speed at which the drone can fly. A response time on the order of 1 s would be desirable if the drone has to cover large areas, as it could fly at a reasonably high speed of 5 m/s and still produce maps with a spatial resolution of 5 m. Currently, the response time of most e-noses is dominated by the filling time of the sensing chamber and the slow recovery time of MOX and electrochemical sensors. The design of a miniaturized chamber in combination with a high flow rate pump is the most straightforward method to improve the response time. The size of the sensing chamber is often limited by the footprint of the sensors used, so using sensors with small footprint (e.g., MEMS) whenever possible is convenient. The housing of the sensors is also another factor affecting the response time of the sensors, so removing the sensor cap typically improves the response time considerably (Burgues et al., 2019). Beyond
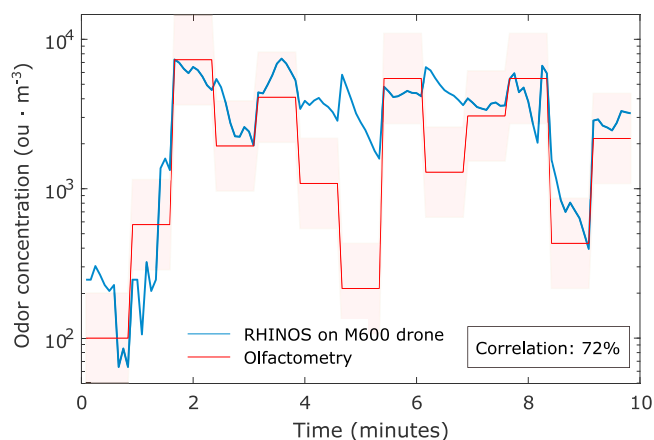


**Figure 12. Real-time odor prediction from the RHINOS on board of the DJI Matrice 600 drone compared to parallel dynamic olfactometry measurements**
The 95% confidence interval of dynamic olfactometry measurements is represented as a shadow rectangle.

CellPress
OPEN ACCESS

that, the response time of low-cost gas sensors can be further improved by signal processing (Di Lello et al., 2014; Fonollosa et al., 2015; Martinez et al., 2019; Pardo et al., 1998).

## STAR★METHODS

Detailed methods are provided in the online version of this paper and include the following:

- KEY RESOURCE TABLE
- RESOURCE AVAILABILITY
  - Lead contact
  - Materials availability
  - Data and code availability
- METHOD DETAILS
  - E-nose fluidic response time
  - E-nose calibration
  - E-nose calibration and validation
  - E-nose validation on the drone

## AUTHOR CONTRIBUTIONS

Conceptualization, all authors; methodology, J.B., M.D.E., S.D., S.M.; software, J.B.; field data acquisition, M.D.E., J.B., S.D.; validation, all authors; formal analysis, J.B. S.M; investigation, J.B.; resources, S.D. and S.M.; data curation, J.B. and M.D.E.; writing—original draft preparation, J.B.; writing—review and editing, all authors; visualization, J.B.; supervision, D.E. and S.M.; project administration, S.D. and S.M.; funding acquisition, S.D. and S.M.

## DECLARATION OF INTERESTS

María Deseada Esclapez and Silvia Doñare are employees of Depuración de Aguas del Mediterraneo (DAM). The authors have previously filed a European patent related to the contents of this work with application number EP21382389.1: "Drone to measure odor concentration".

## REFERENCES

Alferes, J., Adam, G., Delva, J., Noyon, N., Rousseille, F., Cerda, R., Noble, C., and Martin, S. (2017). Advanced on-line monitoring at wastewater treatment plants: coupling e-nose technology and modelling techniques. In 12th IWA Specialized Conference on Instrumentation, Control and Automation.

Alinezhad, E., Haghighi, M., Rahmani, F., Keshizadeh, H., Abdi, M., and Naddafi, K. (2019). Technical and economic investigation of chemical scrubber and bio-filtration in removal of H2S and NH3 from wastewater treatment plant.

J. Environ. Manage. *241*, 32–43. https://doi.org/10.1016/J.JENVMAN.2019.04.003.

Bax, C., Prudenza, S., Gutierrez-Galvez, A., and Capelli, L. (2021). Drift compensation on electronic nose data relevant to the monitoring of odorous emissions from a landfill by Opls. Chem. Eng. Trans. *85*, 13–18.

Bax, C., Sironi, S., and Capelli, L. (2020). How can odors be measured? An overview of methods and their applications. Atmosphere (Basel) *11*, 92.

Bland, J.M., and Altman, D.G. (1999). Measuring agreement in method comparison studies. Stat. Methods Med. Res. *8*, 135–160. https://doi.org/10.1191/096228099673819272.

Boeker, P. (2014). On 'electronic nose'methodology. Sens.Actuators B Chem. *204*, 2–17.

Bottomley, M. (2010). Using automatic odour measurement and dispersion modelling systems as everyday tools within municipal waste treatment. In 15th European Biosolids and

**CellPress** OPEN ACCESS

**iScience** Article

Organic Resources Conference, AquaEnviro., ed. (AquaEnviro).

Bourgeois, W., Romain, A.-C., Nicolas, J., and Stuetz, R.M. (2003). The use of sensor arrays for environmental monitoring: interests and limitations. J. Environ. Monit. *5*, 852–860. https://doi.org/10.1039/b307905h.

Burgués, J., Esclapez, M.D., Doñate, S., Pastor, L., and Marco, S. (2021). Aerial mapping of odorous gases in a wastewater treatment plant using a small drone. Remote Sens. *13*, 1757–1769.

Burgués, J., and Marco, S. (2018). Low power operation of temperature-modulated metal oxide semiconductor gas sensors. Sensors *18*, 339. https://doi.org/10.3390/s18020339.

Burgués, J., and Marco, S. (2020). Environmental chemical sensing using small drones: a review. Sci. Total Environ. *748*, 141172. https://doi.org/10.1016/j.scitotenv.2020.141172.

Burgues, J., Valdez, L.F., and Marco, S. (2019). High-bandwidth e-nose for rapid tracking of turbulent plumes. In ISOEN 2019 - 18th International Symposium on Olfaction and Electronic Nose, Proceedings. https://doi.org/10.1109/ISOEN.2019.8823158.

Campos, J.L., Valenzuela-Heredia, D., Pedrouso, A., Val del Río, A., Belmonte, M., and Mosquera-Corral, A. (2016). Greenhouse gases emissions from wastewater treatment plants: minimization, treatment, and prevention. J. Chem. *2016*, 3796352. https://doi.org/10.1155/2016/3796352.

Cangialosi, F., Intini, G., and Colucci, D. (2018). On line monitoring of odour nuisance at a sanitary landfill for non-hazardous waste. Chem. Eng. Trans. *68*, 127–132.

Capelli, L., Sironi, S., Céntola, P., Del Rosso, R., Il Grande, M., Paolo, C., Del, R., and Il, M. (2008). Electronic noses for the continuous monitoring of odours from a wastewater treatment plant at specific receptors: focus on training methods. Sens. Actuators B Chem. *131*, 53–62. https://doi.org/10.1016/j.snb.2007.12.004.

Capelli, L., Sironi, S., and Del Rosso, R. (2014). Electronic noses for environmental monitoring applications. Sensors *14*, 19979–20007. https://doi.org/10.3390/s141119979.

CEN (2003). DIN EN 13725:2003 Air Quality—Determination of Odour Concentration by Dynamic Olfactometry (BS EN).

Chen, L., Huang, J., and Yang, C.-L. (2001). Absorption of H2S in NaOCl caustic aqueous solution. Environ. Prog. *20*, 175–181. https://doi.org/10.1002/EP.670200313.

Chong, I.-G., and Jun, C.-H. (2005). Performance of some variable selection methods when multicollinearity is present. Chemom. Intell. Lab. Syst. *78*, 103–112.

Cocchi, M., Biancolillo, A., and Marini, F. (2018). Chemometric methods for classification and feature selection. In Comprehensive Analytical Chemistry, J. Jaumot, C. Bedia, and R. Tauler, eds. (Elsevier), pp. 265–299.

De Vito, S., Fattoruso, G., Pardo, M., Tortorella, F., and Di Francia, G. (2012). Semi-supervised learning techniques in artificial olfaction: a novel approach to classification problems and drift counteraction. IEEE Sens. J. *12*, 3215–3224. https://doi.org/10.1109/JSEN.2012.2192425.

Deshmukh, S., Kamde, K., Jana, A., Korde, S., Bandyopadhyay, R., Sankar, R., Bhattacharyya, N., and Pandey, R.A. (2014). Calibration transfer between electronic nose systems for rapid in situ measurement of pulp and paper industry emissions. Anal. Chim. Acta *841*, 58–67. https://doi.org/10.1016/j.aca.2014.05.054.

Dey, A. (2018). Semiconductor metal oxide gas sensors: a review. Mater. Sci. Eng. B Solid-State Mater. Adv. Technol *229*, 206–217. https://doi.org/10.1016/j.mseb.2017.12.036.

Di Carlo, S., and Falasconi, M. (2012). Drift correction methods for gas chemical sensors in artificial olfaction systems: techniques and challenges. In Advances in Chemical Sensors, W. Wang, ed. (Rijeka, Croatia: InTech), pp. 305–326.

Di Lello, E., Trincavelli, M., Bruyninckx, H., and De Laet, T. (2014). Augmented switching linear dynamical system model for gas concentration estimation with MOX sensors in an open sampling system. Sensors (Basel) *14*, 12533–12559. https://doi.org/10.3390/s140712533.

Efron, B., and Gong, G. (1983). A leisurely look at the bootstrap, the jackknife, and cross-validation. Am. Stat. *37*, 36–48.

Fernández, L., Güney, S., Gutierrez-Galvez, A., and Marco, S. (2016). Calibration transfer in temperature modulated gas sensor arrays. Sens. Actuators B Chem. *231*, 276–284.

Fonollosa, J., Fernández, L., Gutiérrez-Gálvez, A., Huerta, R., and Marco, S. (2016). Calibration transfer and drift counteraction in chemical sensor arrays using Direct Standardization. Sens. Actuators B Chem. *236*, 1044–1053. https://doi.org/10.1016/j.snb.2016.05.089.

Fonollosa, J., Sheik, S., Huerta, R., and Marco, S. (2015). Reservoir computing compensates slow response of chemosensor arrays exposed to fast varying gas concentrations in continuous monitoring. Sens. Actuators B Chem. *215*, 618–629. https://doi.org/10.1016/j.snb.2015.03.028.

Franke, W., Frechen, F.-B., and Giebel, S. (2009). H2S, VOC, TOC, electronic noses and odour concentration: use and comparison of different parameters for emission measurement on air treatment systems. Water Sci. Technol. *59*, 1721–1726.

Frechen, F.-B. (2004). Odour emission inventory of German wastewater treatment plants-odour flow rates and odour emission capacity. Water Sci. Technol. *50*, 139–146.

Gardner, J.W., and Bartlett, P.N. (1999). Electronic noses. Principles and applications. Meas. Sci. Technol. *11*, 1087.

González-Sánchez, A., Revah, S., and Deshusses, M.A. (2008). Alkaline biofiltration of H2S odors. Environ. Sci. Technol. *42*, 7398–7404. https://doi.org/10.1021/ES800437F.

Haarstad, K., Bergersen, O., and SÖrheim, R. (2006). Occurrence of carbon monoxide during organic waste degradation. J. Air Waste Manag. Assoc. *56*, 575–580. https://doi.org/10.1080/10473289.2006.10464470.

Haas, T., Lammers, P.S., Diekmann, B., Horner, G., and Boeker, P. (2008). A method for online measurement of odour with a chemosensor system. Sens.Actuators B Chem. *132*, 545–550.

Harreveld, A.P. (2021). Update on the new En13725. Chem. Eng. Trans. *85*, 115–120.

Harvey, D.J., Lu, T.F., and Keller, M.A. (2008). Comparing insect-inspired chemical plume tracking algorithms using a mobile robot. IEEE Trans. Robot. *24*, 307–317. https://doi.org/10.1109/TRO.2007.912090.

Jennings, A., and Cox, A. (2002). Electronic nose technology applied to landfill odors. In 7th Annual Landfill Symposium of the Solid Waste Association of North America (The Solid Waste Association Of North America), pp. 141–151.

Korotcenkov, G., and Cho, B.K. (2011). Instability of metal oxide-based conductometric gas sensors and approaches to stability improvement (short survey). Sens. Actuators B Chem. *156*, 527–538. https://doi.org/10.1016/j.snb.2011.02.024.

Lebrero, R., Bouchy, L., Stuetz, R., and Munoz, R. (2011). Odor assessment and management in wastewater treatment plants: a review. Crit. Rev. Environ. Sci. Technol. https://doi.org/10.1080/10643380903300000.

Lehtinen, J., and Veijanen, A. (2011). Odour monitoring by combined TD–GC–MS–Sniff technique and dynamic olfactometry at the wastewater treatment plant of low H 2 S concentration. Water Air Soil Pollut. *218*, 185–196.

Liu, Q., Li, X., Ye, M., Ge, S.S., and Du, X. (2014). Drift compensation for electronic nose by semi-supervised domain adaption. IEEE Sens. J. *14*, 657–665. https://doi.org/10.1109/JSEN.2013.2285919.

Lochmatter, T. (2010). Bio-Inspired and Probabilistic Algorithms for Distributed Odor Source Localization Using Mobile Robots 4628. https://doi.org/10.5075/epfl-thesis-4628.

Mantovani, A., Artoni, R., Barausse, A., Palmeri, L., Pittarello, A., and Benzo, M. (2011). Modeling odour dispersion from composting plants: comparison with Electronic Nose measurements. Chem. Eng. Trans. *23*, 297–302.

Marco, S., Ortega, A., Pardo, A., and Samitier, J. (1998). Gas identification with tin oxide sensor array and self-organizing maps: adaptive correction of sensor drifts. IEEE Trans. Instrum. Meas. *47*, 316–321.

Martinez, D., Burgués, J., and Marco, S. (2019). Fast measurements with MOX sensors: a least-squares approach to blind deconvolution. Sensors *19*, 4029. https://doi.org/10.3390/s19184029.

Mehmood, T., Liland, K.H., Snipen, L., and Sæbø, S. (2012). A review of variable selection methods in Partial Least Squares Regression. Chemom. Intell. Lab. Syst. *118*, 62–69. https://doi.org/10.1016/j.chemolab.2012.07.010.

Micone, P.G., and Guy, C. (2007). Odour quantification by a sensor array: an application to

## iScience
### Article

landfill gas odours from two different municipal waste treatment works. Sens. Actuators B Chem. *120*, 628–637. https://doi.org/10.1016/j.snb.2006.03.026.

Modla, G., and Lang, P. (2012). Removal and recovery of organic solvents from aqueous waste mixtures by extractive and pressure swing distillation. Ind. Eng. Chem. Res. *51*, 11473–11481. https://doi.org/10.1021/ie300331d.

Munoz, R., Sivret, E.C., Parcsi, G., Lebrero, R., Wang, X., Suffet, I.H.M., and Stuetz, R.M. (2010). Monitoring techniques for odour abatement assessment. Water Res. *44*, 5129–5149.

Naddeo, V., Zarra, T., Giuliani, S., and Belgiorno, V. (2012). Odour impact assessment in industrial areas. Chem. Eng. *30*.

Naddeo, V., Zarra, T., Oliva, G., Kubo, A., Uchida, N., and Higuchi, T. (2016). Odour measurement in wastewater treatment plant by a new prototype of e. nose: correlation and comparison study with reference to both European and Japanese approaches. Chem. Eng. Trans. *54*, 85–90.

Nake, A., Dubreuil, B., Raynaud, C., and Talou, T. (2005). Outdoor in situ monitoring of volatile emissions from wastewater treatment plants with two portable technologies of electronic noses. Sens. Actuators B Chem. *106*, 36–39.

Neumann, P.P., Hernandez Bennetts, V., Lilienthal, A.J., Bartholmai, M., and Schiller, J.H. (2013). Gas source localization with a micro-drone using bio-inspired and particle filter-based algorithms. Adv. Robot. *27*, 725–738. https://doi.org/10.1080/01691864.2013.779052.

Nicolas, J., Romain, A.-C., Wiertz, V., Maternova, J., and Andre, P. (2000). Using the classification model of an electronic nose to assign unknown malodours to environmental sources and to monitor them continuously. Sens. Actuators B Chem. *69*, 366–371.

Olfasense GmbH (2021). EPD Sample Pre-dilution Device.

Oliva, G., Zarra, T., Massimo, R., Senatore, V., Buonerba, A., Belgiorno, V., and Naddeo, V. (2021). Optimization of classification prediction performances of an instrumental odour monitoring system by using temperature correction approach. Chemosensors 9, 147.

Padilla, M., Perera, a., Montoliu, I., Chaudry, A., Persaud, K., and Marco, S. (2010). Drift compensation of gas sensor array data by Orthogonal Signal Correction. Chemom. Intell. Lab. Syst. *100*, 28–35. https://doi.org/10.1016/j.chemolab.2009.10.002.

Palacio, F., Fonollosa, J., Burgués, J., Gómez, J.M., and Marco, S. (2020). Pulsed-temperature metal oxide gas sensors for microwatt power consumption. IEEE Access 8, 70938–70946. https://doi.org/10.1109/ACCESS.2020.2987066.

Pardo, A., Marco, S., and Samitier, J. (1998). Nonlinear inverse dynamic models of gas sensing systems based on chemical sensor arrays for quantitative measurements. IEEE Trans. Instrum. Meas. *47*, 644–651. https://doi.org/10.1109/19.744316.

Park, J.B.K., and Craggs, R.J. (2010). Wastewater treatment and algal production in high rate algal ponds with carbon dioxide addition. Water Sci. Technol. *951*, 633–639. https://doi.org/10.2166/wst.2010.951.

Prata, A.A., Santos, J.M., Timchenko, V., and Stuetz, R.M. (2021). Modelling atmospheric emissions from wastewater treatment plants: Implications of land-to-water roughness change. Sci. Total Environ *792*, 148330. https://doi.org/10.1016/j.scitotenv.2021.148330.

Qu, G., Omotoso, M.M., El-Din, M.G., and Feddes, J.J.R. (2008). Development of an integrated sensor to measure odors. Environ. Monit. Assess. *144*, 277–283.

Romain, A.-C., Nicolas, J., Cobut, P., Delva, J., Nicks, B., and Philippe, F.-X. (2013). Continuous odour measurement from fattening pig units. Atmos. Environ. *77*, 935–942.

Rudnitskaya, A. (2018). Calibration update and drift correction for electronic noses and tongues. Front. Chem. 6, 433. https://doi.org/10.3389/fchem.2018.00433.

Schauberger, G., Piringer, M., Knauder, W., and Petz, E. (2011). Odour emissions from a waste treatment plant using an inverse dispersion technique. Atmos. Environ. *45*, 1639–1647. https://doi.org/10.1016/j.atmosenv.2011.01.007.

Schwarzböck, Therese (2012). Market Review on Available Instruments for Odour Measurement (Berloin: Kompetenz Zentrum Wasser), pp. 1–46. https://publications.kompetenz-wasser.de/pdf/Schwarzböck-2012-492.pdf.

Schwarzböck, T., Frey, M., Rouault, P., Skirlo, H., Giebel, S., Frechen, F.-B., Schmitt, R., Waschnewski, J., and Hartmann, A. (2012). Can electronic noses be used to control odour abatement measures in sewers?–approach by testing 4 multigas-sensor systems under realistic conditions. Chem. Eng. Trans. *30*, 127–132.

Sironi, S., Capelli, L., Céntola, P., and Del Rosso, R. (2007). Development of a system for the continuous monitoring of odours from a composting plant: focus on training, data processing and results validation methods. Sens. Actuators B Chem. *124*, 336–346. https://doi.org/10.1016/j.snb.2006.12.037.

Stuetz, R.M., Engin, G., and Fenner, R.A. (1998). Sewage odour measurements using a sensory panel and an electronic nose. Water Sci. Technol. *38*, 331–335.

Stuetz, R.M., Fenner, R.A., and Engin, G. (1999). Assessment of odours from sewage treatment works by an electronic nose, H2S analysis and olfactometry. Water Res. *33*, 453–461.

Stuetz, R.M., and Frechen, F.-B. (2001). Odours in Wastewater Treatment (IWA Publishing).

Van Harreveld, A.P. (2012). The need for continuous odour monitoring techniques in odour management and currently available technical solutions. Chem. Eng. Trans. *30*.

Wang, C., Yin, L., Zhang, L., and Gao, R. (2010). Metal oxide gas sensors: sensitivity and influencing factors. Sensors *10*, 2088–2106. https://doi.org/10.3390/s100302088.

Wold, S., Ruhe, A., Wold, H., and Dunn, W.J., III (1984). The collinearity problem in linear regression. The partial least squares (PLS) approach to generalized inverses. SIAM J. Sci. Stat. Comput. *5*, 735–743.

Yan, K., and Zhang, D. (2016). Calibration transfer and drift compensation of e-noses via coupled task learning. Sens. Actuators B Chem. *225*, 288–297. https://doi.org/10.1016/j.snb.2015.11.058.

Yi, R., Yan, J., Shi, D., Tian, Y., Chen, F., Wang, Z., and Duan, S. (2021). Improving the performance of drifted/shifted electronic nose systems by cross-domain transfer using common transfer samples. Sens. Actuators B Chem. *329*, 129162. https://doi.org/10.1016/j.snb.2020.129162.

Zarra, T., Galang, M.G., Ballesteros, F., Jr., Belgiorno, V., and Naddeo, V. (2019). Environmental odour management by artificial neural network–A review. Environ. Int. *133*, 105189.

Zarra, T., Galang, M.G.K., Ballesteros, F.C., Belgiorno, V., and Naddeo, V. (2021). Instrumental odour monitoring system classification performance optimization by analysis of different pattern-recognition and feature extraction techniques. Sensors 21, 114.

Zarra, T., Naddeo, V., Belgiorno, V., Reiser, M., and Kranert, M. (2008). Odour monitoring of small wastewater treatment plant located in sensitive environment. Water Sci. Technol. *58*, 89–94.

Zhang, L., Zhang, D., Yin, X., and Liu, Y. (2016). A novel semi-supervised learning approach in artificial olfaction for E-nose application. IEEE Sens. J. *16*, 4919–4931. https://doi.org/10.1109/JSEN.2016.2551743.

Zhu, X., and Goldberg, A.B. (2009). Introduction to semi-supervised learning. Synth. Lect. Artif. Intell. Mach. Learn. *3*, 1–130.

Ziyatdinov, A., Marco, S., Chaudry, A., Persaud, K., Caminal, P., and Perera, A. (2010). Drift compensation of gas sensor array data by common principal component analysis. Sens. Actuators B Chem. *146*, 460–465. https://doi.org/10.1016/j.snb.2009.11.034.

# STAR★METHODS

## KEY RESOURCE TABLE

| REAGENT or RESOURCE | SOURCE | IDENTIFIER |
|---|---|---|
| Software and algorithms | | |
| MATLAB | https://www.mathworks.com | Version R2019b |
| PLS toolbox | https://eigenvector.com | Version 8.7 |

## RESOURCE AVAILABILITY

### Lead contact

Further information and requests for resources and/or reagents should be directed to and will be fulfilled by Prof. Santiago Marco with email: smarco@ibecbarcelona.eu.

### Materials availability

This study did not generate new unique reagents.

### Data and code availability

**Code**: There are restrictions to the availability of code due to intellectual property policies by Depuración de Aguas del Mediterraneo.

**Dataset**. There are restrictions to the availability of experimental dataset due to intellectual property policies by Depuración de Aguas del Mediterraneo

**Additional information**: Any additional information required to reanalyze the data reported in this paper is available from the lead contact upon request.

## METHOD DETAILS

### E-nose fluidic response time

A key parameter of the fluidic system for real-time odor measurements is the time required for filling and cleaning the sensing chamber. To characterize the fluidic time response inside the chamber we used a fast-response photo-ionization detector (PID) with a bandwidth of 300 Hz (miniPID 200B, Aurora Scientific, Canada) to monitor the exhaust of the gas chamber when odor bags of different concentration were connected to the inlet of the e-nose.

### E-nose calibration

For e-nose calibration we used the methodology defined by Capelli et al. (Capelli et al., 2008). Odor samples collected at the emission sources are first analyzed by dynamic olfactometry, and the remaining content in the bags is diluted at several factors to produce additional samples that serve to evaluate the e-nose response in the lower concentration range. The odor concentration of these samples is equal to the dilution factor multiplied by the concentration of the original bag (Micone and Guy, 2007). In our case, we used a pre-dilution device (EPD, Olfasense) with two dilution factors (1/10 and 1/100) and standard deviation in the dilution factor smaller than 5% (Olfasense GmbH, 2021). A third dilution factor 1/1000 was possible by diluting a 1/100 sample with a factor 1/10. A quick analysis of the sensor responses to the diluted samples of the first campaign revealed that it was meaningless to dilute samples beyond 50 $ou_E \cdot m^{-3}$, as this is approximately the limit of detection (LOD) we observed in the e-nose signals. In a typical calibration experiment, the e-nose is brought to the dynamic olfactometry laboratory and warmed up for approximately 1 h. The human panel first analyzes the original odor bags, and the remaining content in the bags after the analysis is used to produce diluted samples. After these dilutions most of the original bags still had some content left that could be used for e-nose exposure. The original bags and their diluted versions is what we call the calibration samples. These samples were presented to the e-nose in duplicate, first in random order and then in decreasing and increasing order to check for a potential memory effect. Each exposure lasted

# iScience
## Article

**CellPress**
OPEN ACCESS

for approximately 5 min, except for high concentration samples (i.e. $>10^4 ou_E \cdot m^{-3}$) where the exposure time was increased to 10 min to ensure that all sensor responses will reach the steady-state. The 21 sensor values at the end of the exposure of each sample were the features used for model building. Blank samples were interleaved between consecutive odor samples to let the sensors recover their baseline. The drift of the sensor baseline between measurement campaigns was compensated by an additive correction based on the response to a blank sample measured at the beginning of each campaign. A typical data collection experiment took approximately 5 h, and the same process was repeated in each measurement campaign.

Partial least-squares regression (PLSR) (Wold et al., 1984) was the calibration model selected for predicting the odor concentration based on the sensor signals, due to its proven robustness against multicollinearity present in e-nose signals and its widespread use for multivariate data analysis in chemometrics. We used MATLAB R2019b and the PLS toolbox 8.7 (Eigenvector Technologies, Manson, USA) for PLS modeling. The logarithm was applied to the predictors (sensor data) and the predictand (odor concentration) to reduce non-linearities and dynamic range of the input data.

The first two campaigns were used for model optimization and the third one for external model validation. Model optimization was based on $k$-fold cross-validation (CV) (Efron and Gong, 1983) with $k=5$. In each fold, the available samples are split into two disjoint subsets: training and test. The training subset is used to build models with different number of latent variables (LVs), and the test subset is used to evaluate the performance of the models. We ensured that diluted samples coming from the same original bag were always in the same data split as the original sample, as these are not independent samples. Thus, we avoided using an original sample in the training set and its diluted version in the test set, as this will result in overoptimistic performance and overfitting. The performance of the models during optimization was evaluated through the root mean squared error in cross-validation (RMSECV). The RMSECV is the average RMSE across the five CV folds, where the RMSE is computed as indicated in Equation 1:

$$RMSE = \sqrt{\frac{1}{n} \sum_{i=1}^{n} (y_i - \widehat{y}_i)^2}$$ (Equation 1)

where $n$ denotes the number of samples, and $y_i$ and $\widehat{y}_i$ are the true and predicted concentration for sample $i$, respectively. Because in our case the predictions and the ground truth are in logarithmic scale, the RMSE in Equation 1 represents a ratio of the original quantities (remember that $\log_{10}(A)-\log_{10}(B) = \log_{10}(A/B)$). Therefore, we can express $10^{RMSE}$ as a relative error ratio. The "knee" in the plot of the RMSECV as a function of the number of LVs was used to determine the optimum number of LV of the PLSR model. After that, the model was refit using the optimum number of LVs and all calibration samples. ctand (odor concentration) to reduce non-linearities and dynamic range of the input data.

In order to study which sensors are more relevant for the PLSR model predictions, we used the variable importance in projection (VIP) scores (Chong and Jun, 2005). VIP is a variable selection method that falls within the category of filter methods (Mehmood et al., 2012). Filter methods assess the importance of the predictors after model building and are generally implemented by defining a ranking criterion and applying a threshold. The advantage of filter methods over wrapper or embedded methods is that they do not require additional validation nor increase the adjustable model parameters (Cocchi et al., 2018). They are also preferred when there are a limited number of samples or the goal is model interpretation rather than obtaining the maximum possible performance. The idea behind the VIP measure is to accumulate the importance of each predictor, $j$, being reflected by the loading weights, $w$, for each component of the model. The VIP measure for the $j$th predictor, $v_j$, is defined as

$$v_j = \sqrt{p \sum_{a=1}^{A} \left[ SS_a (w_{aj}/w_a)^2 \right] \Big/ \sum_{a=1}^{A} SS_a}$$ (Equation 2)

where $p$ is the number of predictors, $SS_a$ is the sum of squares explained by the $a$th component of the model, and $(w_{aj}/w_a)^2$ represents the importance of the $j$th predictor in the $a$th component. By definition, the sum of squared VIP scores is equal to the number of predictors. Therefore, it is common to use as a threshold a VIP score greater than 1 (i.e., larger than the average of squared VIP values), which means that a selected variable will have an above-average influence on the model (Chong and Jun, 2005; Cocchi et al., 2018). This criterion is very reasonable to discard irrelevant variables, while it may have drawbacks if

**CellPress**
OPEN ACCESS

*iScience*
Article

used for assessing the significance of features (Cocchi et al., 2018); A predictor with a VIP score greater than 1 (one) can be considered important in a PLSR model.

### E-nose calibration and validation

The third measurement campaign was used to externally validate the final calibration model with future (unseen) samples. External validation with future samples is the only possible way to obtain a reliable characterization of the e-nose performance due to the well-known issues of sensor drift, cross-sensitivity to weather conditions, and temporal variability of odor emissions. This has been highlighted in two important critique studies of the e-nose field (Boeker, 2014; Franke et al., 2009). Even with external validation samples, it is not trivial how to compare the e-nose predictions to a reference technique (dynamic olfactometry) that has large uncertainty. The most immediate approach is to compute the RMSEP (Equation 1) of the predictions of external validation samples using dynamic olfactometry as ground truth. However, we must differentiate between the *real* odor concentration and the odor concentration measured by olfactometry, which has a large error that is typically quantified as a factor two of the true value (Boeker, 2014). When calibrating an IOMS with dynamic olfactometry, this is a lower bound for the model uncertainty. This is very different from traditional calibration, where known quantities are measured by a new method and the result compared with reference measurements made by a highly accurate method. Therefore, the common approach of comparing e-nose predictions to dynamic olfactometry based on the coefficient of determination (R-squared) or the correlation coefficient ($r$) is not recommended.

Instead, a very popular alternative to compare two measurement methods and evaluate if the new method can replace the old one is the Bland-Altman plot (Bland and Altman, 1999). Bland-Altman methodology was specifically designed to compare a new measurement technique with an established technique that is not free of error. A plot of the differences between the output of the two methods versus the average value of the measurements by both methods allows identification of any systematic difference between the measurements (i.e., fixed bias) or possible outliers. The mean difference is the estimated bias, and the standard deviation of the differences measures the random fluctuations around this mean. Bland-Altman provides expressions for the so-called limits of agreement (LoA) at the 95% confidence level. The main question for the final user is if the LoA are below a pre-established limit of acceptance. In our case, we used the RMSEP and the LoA to quantify the performance of the PLSR model.

### E-nose validation on the drone

In the third campaign, we also performed validation measurements with the drone in flying conditions. Field validation is the only possible way to prove the usefulness of an instrument that will be operated in the field. For that, we equipped the drone with the RHINOS e-nose) and made it hover at various heights above the selected emission sources for around 1 min, with the RHINOS e-nose providing an odor concentration estimate every 5 s. Parallel olfactometric samples were taken during this one-minute period for comparison. Since the e-nose generates 12 predictions in one minute but only a single olfactometric measurement is obtained during the same period, the comparison between both methods is not straightforward. As a workaround, we assessed the e-nose performance based on the percentage of time that the e-nose predictions fell within the uncertainty bands of the olfactometric measurements.